Multifunctional Effects of Green Synthesized Silver Nanoparticles on Glioblastoma Multiform Cancer Cells

Nima Hoseinizadeh[1], Farzaneh Kiarad[1], Zahra Kiani [2,3], Abolfazl Sadeghi[1], Azadeh Taherpour [1,4], Mehdi Shakibaie [3,5*]

[1]*Student research committee, Birjand University of Medical Sciences, Birjand, Iran*

[2] *Department of Pharmacology, School of Pharmacy, Birjand University of Medical Sciences, Birjand, Iran*

[3]*Pharmaceutical Sciences Research Center, Birjand University of Medical Sciences, Birjand, Iran*

[4]*Cellular and Molecular Research Center, Department of Molecular Medicine, Birjand University of Medical Sciences, Birjand, Iran*

[5]*Department of Pharmaceutics and Nanotechnology, School of Pharmacy, Birjand University of Medical Sciences, Birjand, Iran*

[*] Corresponding Author: Tel: +98 5632381924

Email address:

m.shakibaie@bums.ac.ir

[DOI: 10.22068/ijmse.4109]

[*] Corresponding Author: Tel: +98 5632381924
Email address: m.shakibaie@bums.ac.ir

Abstract

Glioblastoma multiforme is an aggressive brain tumor with limited therapeutic options. This study evaluated the multifunctional anticancer effects of curcumin-synthesized silver nanoparticles (curcumin-AgNPs) on the U-87 glioblastoma cell line. Curcumin-AgNPs were biosynthesized using curcumin as a reducing and stabilizing agent and characterized by ultraviolet–visible spectroscopy (UV–Vis), dynamic light scattering (DLS), and transmission electron microscopy (TEM). Cytotoxicity was assessed by MTT assay. The mRNA expression of apoptosis- and epithelial–mesenchymal transition (EMT)-related genes was quantified by real-time PCR. DLS and TEM analyses revealed curcumin-AgNPs with sizes of 56.27±4.59 nm and 22±3 nm, respectively. Curcumin-AgNPs reduced U-87 MG cell viability in a dose- and time-dependent manner. Analysis of apoptosis-related genes showed an increased *BAX/BCL2L1* ratio. Additionally, *FN1* and *VIM* were downregulated to 0.48- and 0.60-fold, respectively, indicating inhibitory effects on EMT and the metastatic potential of U-87 MG cells. These findings indicated that curcumin-AgNPs exhibit cytotoxic, pro-apoptotic, and EMT-modulating effects in U-87 MG cells, highlighting their potential as a multifunctional nanoplatform for glioblastoma research. Further studies are required to elucidate their underlying mechanisms.

***Keywords*:** anti-cancer; glioblastoma; silver nanoparticles; curcumin; EMT; migration.

[DOI: 10.22068/ijmse.4109]

1. INTRODUCTION

Glioblastoma multiforme (GBM), a type of astrocytoma, is the most common primary CNS malignancy. It's a fast-growing tumor that spreads into neighboring normal brain tissue and is one of the most lethal cancers worldwide [1]. Brain tumors are divided into four grades (I to IV scale) based on their fast growth. Grade IV brain tumors are the most aggressive GBMs at this grade. These tumors are rarely cured, but proper treatment can increase the life expectancy of patients [2].

The use of new methods in cancer treatment has significantly increased the rate of recovery from this disease. New approaches in cancer treatment have greatly benefited from nanotechnology [3]. Among the nanostructures, metal nanoparticles play a significant role in cancer treatment and diagnosis [4]. Silver nanoparticles (AgNPs), as one of the metal nanoparticles, have a bright future in medical applications [5].

Different physical, chemical, and biological methods are used to synthesize AgNPs, but green synthesis methods have been essential due to their biocompatibility [6]. In green synthesis methods, herbal extracts are used for the synthesis of nanoparticles, which have many advantages, such as lower cost, compatibility with the environment, and the possibility of easy production on a large scale [7]. A method for green chemistry synthesis of AgNPs using curcumin as a reducing agent can improve the biological effect of nanoparticles [8].

Several studies have demonstrated that green-synthesized AgNPs inhibited cancer cell growth by generating intracellular reactive oxygen species (ROS), modulating apoptosis-related proteins (e.g., caspase-3, -8, -9), and inducing cell death in glioblastoma and other cancer models [9, 10]. Moreover, the combination of AgNPs with cisplatin has been demonstrated to enhance glioblastoma cell death through transient receptor potential melastatin 2 (TRPM2) activation [11]. Curcumin itself exhibits anticancer activity by regulating multiple signaling pathways involved in proliferation, migration, invasion, and cell death [12]. It modulates PI3K/AKT/mTOR, NF-κB, and SHH/GLI1 pathways and induces apoptosis by downregulating anti-apoptotic proteins such as BCL-XL [13-15]. In addition, curcumin has been reported to suppress epithelial mesenchymal transition (EMT) by downregulating N-cadherin and vimentin expression in cancer cells [16].

Despite these promising findings, the potential of curcumin-mediated green-synthesized AgNPs has not yet been systematically investigated in U-87 MG cells, particularly with respect to their effects on viability, migration, and the expression of apoptosis- and EMT-related genes. To address

[DOI: 10.22068/ijmse.4109]

this gap, in the current study we synthesized spherical curcumin-AgNPs with a suitable size for potential blood-brain barrier (BBB) penetration and evaluated their multifunctional anticancer effects using MTT assay, wound-healing assay, and quantitative real-time PCR.

2. EXPERIMENTAL PROCEDURES

2.1.Materials

Dulbecco's modified Eagle's medium (DMEM), fetal bovine serum (FBS), streptomycin, penicillin, and trypsin were obtained from GIBCO (InvitrogenTM, Grand Island, USA). 3-[4,5-dimethylthiazol-2-yl]-2,5-diphenyltetrazolium bromide (MTT) was purchased from Sigma-Aldrich (St. Louis, MO, USA). All other chemical reagents used in buffer preparation and solution were purchased from the Merck company (Hohenbrunn, Germany). Silver nitrate and curcumin were purchased from Samchun (Pure Chemical Co., Ltd.).

2.2.Green Synthesized of Silver Nanoparticles

AgNPs were synthesized as described previously [17]. Briefly, 50 µM of curcumin was achieved by dissolving it in deionized water, and the pH was then adjusted to 8. The solution was heated to 70°C and, under vigorous stirring, an aqueous solution of 4 mM silver nitrate was added dropwise (1:15 ratio). The reaction was allowed to proceed for 2 h. Nanoparticles were collected by centrifugation at 12,000 rpm for 5 min; the pellet was washed three times with deionized water to remove unreacted curcumin and impurities. Finally, the nanoparticles were resuspended in deionized water and stored at 4°C until use.

2.3. Characterization of Silver Nanoparticles

2.3.1. Ultraviolet-Visible Analysis

Ultraviolet-visible (UV–Vis) spectroscopy was used to evaluate the optical properties of synthesized AgNPs. For this purpose, the adsorption spectrum of colloidal solution of nanoparticles in the range of 300 to 600 nm was measured using a spectrophotometer (BioTek Epoch, USA).

2.3.2. Dynamic Light Scattering

[DOI: 10.22068/ijmse.4109]

The nanoparticles were diluted to an aqueous solution at room temperature, and the hydrodynamic diameter and zeta potential of the nanoparticles were measured using a dynamic light scattering (DLS) instrument (Brookhaven, USA).

2.3.3. Transmission Electron Microscopy

The morphology of the curcumin-AgNPs was examined using a transmission electron microscope (TEM, model Zeiss-EM10C, Germany) operating at an accelerating voltage of 100 kV. For sample preparation, a drop of the nanoparticle suspension was placed onto a carbon-coated copper grid (200-mesh) and air-dried prior to imaging.

2.4. Cell Culture and Media

The human GBM cell line U-87 MG was obtained from the Iranian Biological Resource Center (Tehran, Iran). The cells were cultured in a T-75 culture flask containing a basal medium comprised of DMEM supplemented with 10 % (v/v) FBS, 100 µg/ml streptomycin, and 100 IU/ml penicillin. The cell culture flasks were maintained in a humidified incubator at 5 % CO_2 and 37°C.

2.4.1. Evaluation of Cytotoxicity

The cells were removed from the T-75 culture flask using trypsin solution (0.25% w/v) after a cultivation time of 72 h. The suspended cells were precipitated by centrifuge at 250 g for 5 min. The settled U-87 MG cells were resuspended in basal medium and added at the same seeding density (10000 cells/ cm^2) in a flat-bottom 96-well plate. Cell viability was determined by the MTT assay using the direct method. The cytotoxicity effect of curcumin-AgNPs on U-87 MG cells was analyzed at different concentrations (1-10 µg/ml) over the culture period. Untreated cells served as the control group. After 48 and 72 h of incubation, MTT solution (5 mg/ml in PBS) was added to each well of the 96-well plate and incubated for 4 h at 37 °C in a humidified atmosphere (95% air, 5% CO_2) in the dark. Following removal of the MTT solution, DMSO was added to each well. Subsequently, the optical density of the cells was measured by a multiwell scanning spectrophotometer at wavelengths 570 and 630 nm.

2.4.2. Real-Time Polymerase Chain Reaction

[DOI: 10.22068/ijmse.4109]

After removing the culture medium from a 6 cm² dish, the cells were washed twice with PBS. The cells were removed from the culture dishes using trypsin solution (0.25% w/v) after a cultivation time of 48 h. The suspended cells were precipitated by centrifuge at 250 g for 5 min. Cell pellets were resuspended with 200 µl PBS and kept at -80ºC for RNA extraction. Total RNA was extracted by a highly pure RNA isolation kit (Roche Applied Science, Germany) according to the manufacturer's instructions. The RNA quality and quantity were measured using a Nanodrop spectrophotometer (Thermo Fisher Scientific). The synthesis of cDNA from an RNA template was performed using the RevertAid First Strand cDNA Synthesis Kit (Thermo Fisher Scientific) according to the manufacturer's instructions. Primer sequences applied in real-time PCR were listed in Table 1. qRT-PCR analysis was conducted by the Applied Biosystems StepOne^{TM} 48-Well Real-Time PCR System and SYBR® Green Real-Time PCR Master Mix (Applied Biosystems). Relative quantification was performed using the comparative Ct ($2^{-\Delta\Delta Ct}$) method, and *HPRT1* was considered a reference gene.

<Table 1>

2.4.3. Wound Healing Assay

Cancer cell migration was analyzed by wound-healing assay. The cells were seeded in a 3.5 cm^2 culture dish and cultured until the confluency of the cells reached 95%. The culture dish was scratched across the surface of the cancer cell monolayer with a 100 µl sterile pipette tip and washed with PBS three times to remove cell debris. After scratching, the cells were maintained in reduced-serum medium (1% FBS) to minimize proliferation and allow migration to be evaluated. The treated group received 2 µg/ml curcumin-AgNPs, while untreated scratched cells served as the control group. The wound area was visualized and photographed by an inverted microscope 8 h after incubation in a humidified incubator at 5 % CO_2 and 37°C.

3.5. Statistical Analysis

Statistical analyses were performed with SPSS software (version 16). All data are presented as mean ± standard deviation (SD). Differences between groups in the wound healing test were evaluated using the independent-sample t-test. The relative expression levels of target genes were analyzed using REST 2009 software (version 2.0.13). A p-value of <0.05 was considered statistically significant.

[DOI: 10.22068/ijmse.4109]

3. RESULTS AND DISCUSSION

3.1. Morphological and Physicochemical Characterization of Curcumin-Silver Nanoparticles

Nanomedicine provides new strategies to tackle human diseases at the nanoscale level, where most biological molecules exist and function. Comprehensive physicochemical characterization of nanomaterials is essential in biomedical research to accurately interpret their biological effects. Key parameters such as morphology, particle size, purity, hydrodynamic diameter, aggregation, and stability in aqueous media are routinely assessed for nanoparticle characterization [18]. In the present study, UV-Vis spectroscopy, DLS, and TEM techniques were employed to characterize curcumin-AgNPs. The UV-Vis spectrum of curcumin-AgNPs displayed a characteristic plasmonic absorption peak at 410 nm, confirming the successful synthesis of AgNPs with high purity (**Fig. 1**). DLS analysis revealed an average particle size of 56.27±4.59 nm. Notably, after four months of storage, the size only slightly increased to 61.88±2.76 nm, indicating excellent colloidal stability. The zeta potential of -21 mV further supported the stability of the nanoparticles. TEM imaging showed that the curcumin-AgNPs were predominantly spherical with an average diameter of 22±3 nm. The smaller size observed by TEM compared to DLS is consistent with the hydrodynamic nature of DLS measurements. These findings confirm the successful biosynthesis of small, stable, and monodispersed curcumin-AgNPs. The particle size obtained falls within the optimal range for biomedical applications, including potential BBB penetration [19]. Similar physicochemical features have been reported in earlier studies on plant-mediated nanoparticles [20, 21].

<Fig. 1>

3.2. Cytotoxic Effect of Curcumin-Silver Nanoparticles

The results showed that the cytotoxic effects of curcumin-AgNPs on U-87 MG cells were both time- and dose-dependent. As shown in **Fig. 2** (**A**, **B**), after 48 h of treatment, cell viability

[DOI: 10.22068/ijmse.4109]

decreased progressively from 97.67% at 1 µg/ml to 25.85% at 10 µg/ml. Specifically, at 2 µg/ml, cell viability was 89.39% after 48 h, indicating only a mild reduction compared to the control. At 72 h, a further reduction was observed, with cell viability decreasing from 87.05% at 1 µg/ml to 8.93% at 10 µg/ml. For downstream experiments, a sublethal concentration (2 µg/ml at 48 h) was selected to minimize excessive cytotoxicity and allow investigation of cellular responses under sublethal conditions.

<**Fig. 2**>

Consistent with our findings, Karan et al. (2022) demonstrated that curcumin-AgNPs exhibited potent cytotoxic effect against DLD-1 and A549 cancer cell lines, with ~80% lethality at 1.0 mg/ml after 24 h [22]. Similarly, several reports have shown the anti-proliferative activity of green-synthesized AgNPs in diverse cancer types, including breast, pancreatic, lung, prostate, gastric, colon, and liver cancers [23-25]. However, studies investigating their effects on glioblastoma remain limited. For instance, Eugenio et al. (2018) evaluated the effects of Ag/AgCl-NPs biogenically synthesized using yeast culture on GBM02 glioma cells and reported that these nanoparticles reduced proliferation more efficiently than TMZ at high concentrations [26]. Similarly, Simsek et al. (2021) used extract from *Lavandula angustifolia* to study the green synthesis of AgNPs and confirmed their anti-proliferative activity in U-87 MG cells [27]. To the best of our knowledge, the present study is the first to evaluate curcumin-AgNPs in U-87 MG cells.

3.3. Apoptotic Effect of Curcumin-Silver Nanoparticles

A large number of genes are involved in the induction of apoptosis. Of these, members of the BCL-2 gene family play an effective role. The proapoptotic gene *BAX* promotes apoptosis, while the anti-apoptotic gene *BCL-XL* prevents it. In the curcumin-AgNP-treated U-87 MG cells, *BAX* expression increased 2.21-fold, whereas *BCL2L1* expression showed only a slight rise of 1.1-fold, as revealed in **Fig. 3**. Consequently, the *BAX/BCL2L1* ratio increased nearly 2-fold compared to the control, indicating a clear shift toward apoptosis induction.

<**Fig. 3**>

[DOI: 10.22068/ijmse.4109]

Apoptosis or programmed cell death is a gene-regulated phenomena relevant in both physiological and pathological circumstances. Death receptors, mitochondrial responses, caspase activation, and the regulation of BCL2 and BAX gene expression are significant guiding mechanisms of apoptosis [28]. The induction of apoptosis in tumor cells is considered a valuable strategy in both cancer prevention and therapy [29]. In current study, the apoptotic effect of curcumin-AgNPs was examined through the relative ratio of *BAX* to *BCL2L1* in U-87 MG cells after 48 h of treatment. Our results revealed an increase in the *BAX/BCL2L1* ratio. Numerous studies have demonstrated that nanoparticles can induce apoptosis in various tumor models. For example, Bin-Jumah et al. (2020) synthesized AgNPs via an eco-friendly approach using *Beta vulgaris* root extracts and demonstrated an increased BAX/BCL2 protein ratio in HUH-7 hepatic cells [30]. Similarly, Baharara et al. reported that AgNPs induced apoptosis in MCF-7 cells through the regulation of *BAX* and *BCL2* expression as well as activation of *caspases-3* and *-9* [28]. Urbańska et al. (2015) also studied the impact of AgNPs on GBM proliferation and apoptosis using an *in ovo* model, concluding that the antiproliferative properties predominated over their pro-apoptotic effects [31]. How apoptosis is triggered may depend on cell type, the nature of the induced damage, and chemical characteristics of nanoparticles [32].

3.4. EMT-Modulating Effect of Curcumin-Silver Nanoparticles

EMT is characterized by decreased expression of epithelial markers and increased expression of mesenchymal markers. To assess the effect of curcumin-AgNPs on EMT, U-87 MG cells were treated with 2 µg/ml NPs, and the expression of EMT-related genes was analyzed. As shown in **Fig. 4**, the expression level of *CDH2* (N-cadherin) exhibited slight changes, which was not statistically significant. In contrast, *FN1* (fibronectin) and *VIM* (vimentin) were significantly downregulated to 0.48-fold and 0.60-fold, respectively, in treated U-87 MG cells compared with the control ($p < 0.05$).

<**Fig. 4**>

Beyond apoptosis, another critical mechanism by which nanoparticles affect tumor progression is the regulation of EMT. EMT plays a pivotal role in tumor progression, where polarized epithelial

[DOI: 10.22068/ijmse.4109]

cells transform and acquire mesenchymal-like motility. This process is characterized by the breakdown of cell-cell junctions, loss of epithelial markers like E-cadherin, and the acquisition of mesenchymal markers including N-cadherin, vimentin, and fibronectin [33]. Curcumin has been widely recognized as an inhibitor of EMT, suppressing the invasive potential of oral squamous cell carcinoma by modulating EMT-related pathways [34, 35]. Consistently, Kumari et al. (2017) showed that selenium-curcumin NPs downregulated CD44 and N-cadherin in HCT116 cells, suggesting suppression of EMT, although E-cadherin expression remained unchanged [36]. Decreased CD44 has also been linked with reduced cancer cell proliferation and enhanced apoptosis [37]. In another study, Viswanathan et al. (2023) showed that AuNPs downregulated *VIM* expression and inhibited A549 cell migration [38]. In line with these findings, our results demonstrated that curcumin-AgNPs downregulated *VIM* expression in U-87 MG cells. In contrast, Matysiak-Kucharek et al. (2023) observed that AgNPs increased the expression of mesenchymal EMT markers (*CDH2*, *VIM*, *MMP-2*, *-9*) while reducing epithelial *CDH1* in MDA-MB-436 cells, indicating a potential stimulation of EMT [39].

3.5. Inhibitory Effect of Curcumin-Silver Nanoparticles on Cell Migration

The migration of cancer cells is a key factor in tumor progression. In this study, we examined cell migration using the reliable and most popular in vitro scratch assay on U-87 MG cells. The results showed that treatment with 2 µg/ml curcumin-AgNPs slightly reduced cell migration relative to the control group, although this reduction was not significant at this concentration (**Fig. 5**). Previous reports have also shown that AgNPs impaired cell migration and invasion, including in MCF-7 and 4T1 breast cancer cells [40] and A549 lung cancer cells [41].

<**Fig. 5**>

4. CONCLUSIONS

In summary, this study demonstrates that stable AgNPs are successfully synthesized with curcumin and exhibit multifunctional anticancer effects in U-87 MG cells. Curcumin-AgNPs exerted cytotoxic and pro-apoptotic effects while also modulating EMT-related gene expression. These findings highlight the potential of these nanoparticles as a multifunctional nanotherapeutic platform for glioblastoma research.

[DOI: 10.22068/ijmse.4109]

ACKNOWLEDGEMENTS

This article has been extracted from the thesis written by Nima Hoseinizadeh and Farzaneh Kiarad in the School of Medicine, Birjand University of Medical Sciences (Registration No: 456865).

REFERENCES

1. Wang, Z., Liu, F., Liao, W., Yu, L., Hu, Z., Li, M., and Xia, H., "Curcumin suppresses glioblastoma cell proliferation by p-AKT/mTOR pathway and increases the PTEN expression." Arch. Biochem. Biophys., 2020, 689, 108412.
2. Amer, R. G., Ezz El Arab, L. R., Abd El Ghany, D., Saad, A. S., Bahie-Eldin, N., and Swellam, M., "Prognostic utility of lncRNAs (LINC00565 and LINC00641) as molecular markers in glioblastoma multiforme (GBM)." J. Neurooncol., 2022, 158, 3, 435–444.
3. Liu, D., Dai, X., Ye, L., Wang, H., Qian, H., Cheng, H., and Wang, X., "Nanotechnology meets glioblastoma multiforme: Emerging therapeutic strategies." Wiley Interdiscip. Rev. Nanomed. Nanobiotechnol., 2023, 15, 1, e1838.
4. Gawel, A. M., Singh, R., and Debinski, W., "Metal-based nanostructured therapeutic strategies for glioblastoma treatment—an update." Biomedicines., 2022, 10, 7, 1598.
5. Kovács, D., Igaz, N., Gopisetty, M. K., and Kiricsi, M., "Cancer therapy by silver nanoparticles: fiction or reality?" Int. J. Mol. Sci., 2022, 23, 2, 839.
6. Fahim, M., Shahzaib, A., Nishat, N., Jahan, A., Bhat, T. A., and Inam, A., "Green synthesis of silver nanoparticles: A comprehensive review of methods, influencing factors, and applications." JCIS Open., 2024, 16, 100125.
7. Alharbi, N. S., Alsubhi, N. S., and Felimban, A. I., "Green synthesis of silver nanoparticles using medicinal plants: characterization and application." J. Radiat. Res. Appl. Sci., 2022, 15, 3, 109–124.
8. Karan, T., Erenler, R., and Bozer, B. M., "Synthesis and characterization of silver nanoparticles using curcumin: cytotoxic, apoptotic, and necrotic effects on various cell lines." Z. Naturforsch., 2022.
9. Xu, Z., Feng, Q., Wang, M., Zhao, H., Lin, Y., and Zhou, S., "Green biosynthesized silver nanoparticles with aqueous extracts of ginkgo biloba induce apoptosis via mitochondrial pathway in cervical cancer cells." Front. Oncol., 2020, 10, 575415.
10. Ejidike, I. P., and Clayton, H. S., "Green synthesis of silver nanoparticles mediated by Daucus carota L.: antiradical, antimicrobial potentials, in vitro cytotoxicity against brain glioblastoma cells." Green. Chem. Lett. Rev., 2022, 15, 2, 297–310.

[DOI: 10.22068/ijmse.4109]

11. Akyuva, Y., and Nazıroğlu, M., "Silver nanoparticles potentiate antitumor and oxidant actions of cisplatin via the stimulation of TRPM2 channel in glioblastoma tumor cells." Chem. Biol. Interact., 2023, 369, 110261.
12. Wong, S. C., Kamarudin, M. N. A., and Naidu, R., "Anticancer mechanism of curcumin on human glioblastoma." Nutrients., 2021, 13, 3, 950.
13. Borges, G. A., Elias, S. T., Amorim, B., de Lima, C. L., Coletta, R. D., Castilho, R. M., Squarize, C. H., and Guerra, E. N. S., "Curcumin downregulates the PI3K–AKT–mTOR pathway and inhibits growth and progression in head and neck cancer cells." Phytother. Res., 2020, 34, 12, 3311–3324.
14. Wang, J.-b., Qi, L.-l., Zheng, S.-d., and Wu, T.-x., "Curcumin induces apoptosis through the mitochondria-mediated apoptotic pathway in HT-29 cells." J. Zhejiang. Univ. Sci. B., 2009, 10, 2, 93–102.
15. Du, W. Z., Feng, Y., Wang, X. F., Piao, X. Y., Cui, Y. Q., Chen, L. C., Lei, X. H., Sun, X., Liu, X., and Wang, H. B., "Curcumin suppresses malignant glioma cells growth and induces apoptosis by inhibition of SHH/GLI 1 signaling pathway in vitro and vivo." CNS. Neurosci., 2013, 19, 12, 926–936.
16. Gallardo, M., and Calaf, G. M., "Curcumin inhibits invasive capabilities through epithelial mesenchymal transition in breast cancer cell lines." Int. J. Oncol., 2016, 49, 3, 1019–1027.
17. Taherpour, A., Zarban, A., Asadian, A. H., Karbasi, S., and Shakibaie, M., "Efficacy of curcumin-synthesized silver nanoparticles on MCF-7 breast cancer cells." Med. Oncol., 2025, 42, 7, 265.
18. Akhtar, M. J., Ahamed, M., Kumar, S., Khan, M. M., Ahmad, J., and Alrokayan, S. A., "Zinc oxide nanoparticles selectively induce apoptosis in human cancer cells through reactive oxygen species." Int. J. Nanomedicine., 2012, 7, 845–857.
19. Hersh, A. M., Alomari, S., and Tyler, B. M., "Crossing the Blood-Brain Barrier: Advances in Nanoparticle Technology for Drug Delivery in Neuro-Oncology." Int. J. Mol. Sci., 2022, 23, 8.
20. Keskin, C., Aslan, S., Baran, M. F., Baran, A., Eftekhari, A., Adıcan, M. T., Ahmadian, E., Arslan, S., and Mohamed, A. J., "Green Synthesis and Characterization of Silver Nanoparticles Using Anchusa Officinalis: Antimicrobial and Cytotoxic Potential." Int. J. Nanomedicine., 2025, 20, null, 4481–4502.
21. Rudrappa, M., Rudayni, H. A., Assiri, R. A., Bepari, A., Basavarajappa, D. S., Nagaraja, S. K., Chakraborty, B., Swamy, P. S., Agadi, S. N., Niazi, S. K., and Nayaka, S. "Plumeria alba-Mediated Green Synthesis of Silver Nanoparticles Exhibits Antimicrobial Effect and Anti-Oncogenic Activity against Glioblastoma U118 MG Cancer Cell Line." Nanomaterials., 2022, 12, 3, 493.
22. Karan, T., Erenler, R., and Moran Bozer, B., "Synthesis and characterization of silver nanoparticles using curcumin: cytotoxic, apoptotic, and necrotic effects on various cell lines." Z Naturforsch. C. J. Biosci., 2022, 77, 7-8, 343–350.
23. Nosrati, F., Fakheri, B., Ghaznavi, H., Mahdinezhad, N., Sheervalilou, R., and Fazeli-Nasab, B., "Green synthesis of silver nanoparticles from plant Astragalus fasciculifolius Bioss and evaluating cytotoxic effects on MCF7 human breast cancer cells." Sci. Rep., 2025, 15, 1, 25474.

[DOI: 10.22068/ijmse.4109]

24. Yüce, M., Albayrak, E., Yontar, A. K., Çevik, S., and Gumuskaptan, C., "Eco-friendly synthesis of silver nanoparticles using Anemone coronaria bulb extract and their potent anticancer and antibacterial activities." Sci. Rep., 2025, 15, 1, 32066.
25. Wang, D., Ke, H., Wang, H., Shen, J., Jin, Y., Lu, B., Wang, B., Li, S., Li, Y., Im, W. T., Siddiqi, M. Z., and Zhu, H. "Green Synthesis of Silver Nanoparticles (CM-AgNPs) from the Root of Chuanminshen for Improving the Cytotoxicity Effect in Cancer Cells with Antibacterial and Antioxidant Activities." Molecules., 2024, 29, 23, 5682.
26. Eugenio, M., Campanati, L., Müller, N., Romão, L. F., de Souza, J., Alves-Leon, S., de Souza, W., and Sant'Anna, C., "Silver/silver chloride nanoparticles inhibit the proliferation of human glioblastoma cells." Cytotechnology., 2018, 70, 6, 1607–1618.
27. Simsek, A., Pehlivanoglu, S., and Aydin Acar, C., "Anti-proliferative and apoptotic effects of green synthesized silver nanoparticles using Lavandula angustifolia on human glioblastoma cells." 3 Biotech., 2021, 11, 8, 374.
28. Baharara, J., Namvar, F., Ramezani, T., Mousavi, M., and Mohamad, R. "Silver Nanoparticles Biosynthesized Using Achillea biebersteinii Flower Extract: Apoptosis Induction in MCF-7 Cells via Caspase Activation and Regulation of Bax and Bcl-2 Gene Expression." Molecules., 2015, 20, 2, 2693–2706.
29. Mousavi, S. H., Tavakkol-Afshari, J., Brook, A., and Jafari-Anarkooli, I., "Role of caspases and Bax protein in saffron-induced apoptosis in MCF-7 cells." Food. Chem. Toxicol., 2009, 47, 8, 1909–1913.
30. Bin-Jumah, M., Al-Abdan, M., Albasher, G., and Alarifi, S., "Effects of Green Silver Nanoparticles on Apoptosis and Oxidative Stress in Normal and Cancerous Human Hepatic Cells in vitro." Int. J. Nanomed., 2020, 15, 1537–1548.
31. Urbańska, K., Pająk, B., Orzechowski, A., Sokołowska, J., Grodzik, M., Sawosz, E., Szmidt, M., and Sysa, P., "The effect of silver nanoparticles (AgNPs) on proliferation and apoptosis of in ovo cultured glioblastoma multiforme (GBM) cells." Nanoscale, Res ,Lett., 2015, 10, 98.
32. Chen, L., Wu, L., and Yang, W.-X., "Nanoparticles Induce Apoptosis Via Mediating Diverse Cellular Pathways." Nanomedicine., 2018, 13.
33. Xia, P., "The significance of epithelial–mesenchymal transition (EMT) in the initiation, plasticity, and treatment of glioblastoma." Genes Dis., 2025, 101711.
34. Bahrami, A., Majeed, M., and Sahebkar, A., "Curcumin: A potent agent to reverse epithelial-to-mesenchymal transition." Cell. Oncol., 2019, 42, 405–421.
35. Lee, A. Y.-L., Fan, C.-C., Chen, Y.-A., Cheng, C.-W., Sung, Y.-J., Hsu, C.-P., and Kao, T.-Y., "Curcumin inhibits invasiveness and epithelial-mesenchymal transition in oral squamous cell carcinoma through reducing matrix metalloproteinase 2, 9 and modulating p53-E-cadherin pathway." Integr. Cancer. Ther., 2015, 14, 5, 484–490.
36. Kumari, M., Ray, L., Purohit, M. P., Patnaik, S., Pant, A. B., Shukla, Y., Kumar, P., and Gupta, K. C., "Curcumin loading potentiates the chemotherapeutic efficacy of selenium nanoparticles in HCT116 cells and Ehrlich's ascites carcinoma bearing mice." Eur. J. Pharm. Biopharm., 2017, 117, 346–362.
37. Pi, J., Yang, F., Jin, H., Huang, X., Liu, R., Yang, P., and Cai, J., "Selenium nanoparticles induced membrane bio-mechanical property changes in MCF-7 cells by disturbing membrane molecules and F-actin." Bioorg. Med. Chem. Lett., 2013, 23, 23, 6296–6303.
38. Viswanathan, S., Palaniyandi, T., Chellam, D. C., Ahmed, M. F., Shoban, N., Pushpakumar, M., Abdul Wahab, M. R., Baskar, G., Ravi, M., Sivaji, A., Natarajan, S., and

[DOI: 10.22068/ijmse.4109]

Sankareswaran, S. K., "Anti-cancer activity of Hypnea valentiae seaweed loaded gold nanoparticles through EMT signaling pathway in A549 cells." Biochem. Syst. Ecol., 2023, 107, 104606.
39. Matysiak-Kucharek, M., Sawicki, K., Kurzepa, J., Wojtyła-Buciora, P., and Kapka-Skrzypczak, L., "The influence of silver nanoparticles on the process of epithelial transition in the context of cancer metastases." Med. Pr., 2023, 74, 6, 541–548.
40. Kovács, D., Igaz, N., Marton, A., Rónavári, A., Bélteky, P., Bodai, L., Spengler, G., Tiszlavicz, L., Rázga, Z., Hegyi, P., Vizler, C., Boros, I. M., Kónya, Z., and Kiricsi, M., "Core–shell nanoparticles suppress metastasis and modify the tumour-supportive activity of cancer-associated fibroblasts." J. Nanobiotechnol., 2020, 18, 1, 18.
41. Que, Y. M., Fan, X. Q., Lin, X. J., Jiang, X. L., Hu, P. P., Tong, X. Y., and Tan, Q. Y., "Size dependent anti-invasiveness of silver nanoparticles in lung cancer cells." RSC. Advances., 2019, 9, 37, 21134–21138.

TABLES

Table 1. Primer sequences used in real-time PCR.

Primer	Sequence: 5′ → 3′
HPRT1	ATGCTGAGGATTTGGAAAGGG
	ACAGAGGGCTACAATGTGATGG
BAX	TGCCAGCAAACTGGTGCTC
	AACCACCCTGGTCTTGGAT
BCL2L1	GAGACTCAGTGAGTGAGCAGGTG
	GCTTGTAGGAGAGAAAGTCAACC
VIM	CAGCTAACCAACGACAAAGCCC
	CAGAGACGCATTGTCAACATCC
FN1	TTGTTATGGAGGAAGCCGAGG
	CACCCACTCGGTAAGTGTTCC
CDH2	ACCAGGTTTGGAATGGGACAG
	TGAGGGCATTGGGATCGTCAG

[DOI: 10.22068/ijmse.4109]

[DOI: 10.22068/ijmse.4109]

FIGURE CAPTIONS

Fig. 1. Characterization of curcumin-AgNPs. (**A**), Plasmonic absorption of AgNPs synthesized by curcumin have a peak at 410 nm with OD (optical density) 0.8 (**B**), Particle size distribution by DLS (**C**), TEM image of nanoparticles.

Fig. 2. Cytotoxicity of U-87 MG cells treated with curcumin-AgNPs. (**A**, **B**) Cell viability at 1-10 µg/ml after 48 h and 72 h (*$p < 0.05$, **$p < 0.01$ compared to untreated group).

Fig. 3. Apoptosis-related genes expression in U-87 MG cells treated with curcumin-AgNPs (*$p < 0.05$ compared to untreated group).

Fig. 4. EMT-related gene expression in U-87 MG cells treated with curcumin-AgNPs (*$p < 0.05$, **$p < 0.01$ compared to untreated group).

Fig. 5. Effect of curcumin-AgNPs on U-87 cell migration using Scratch-wound assay. (**A**, **C**) A scratch was made onto a monolayer of untreated U-87 MG cells at 0 h, (**B**) Untreated cells after 8 h, (**D**) treated cells with curcumin-AgNPs after 8 h, (**E**) Quantification of open wound area over time.

[DOI: 10.22068/ijmse.4109]

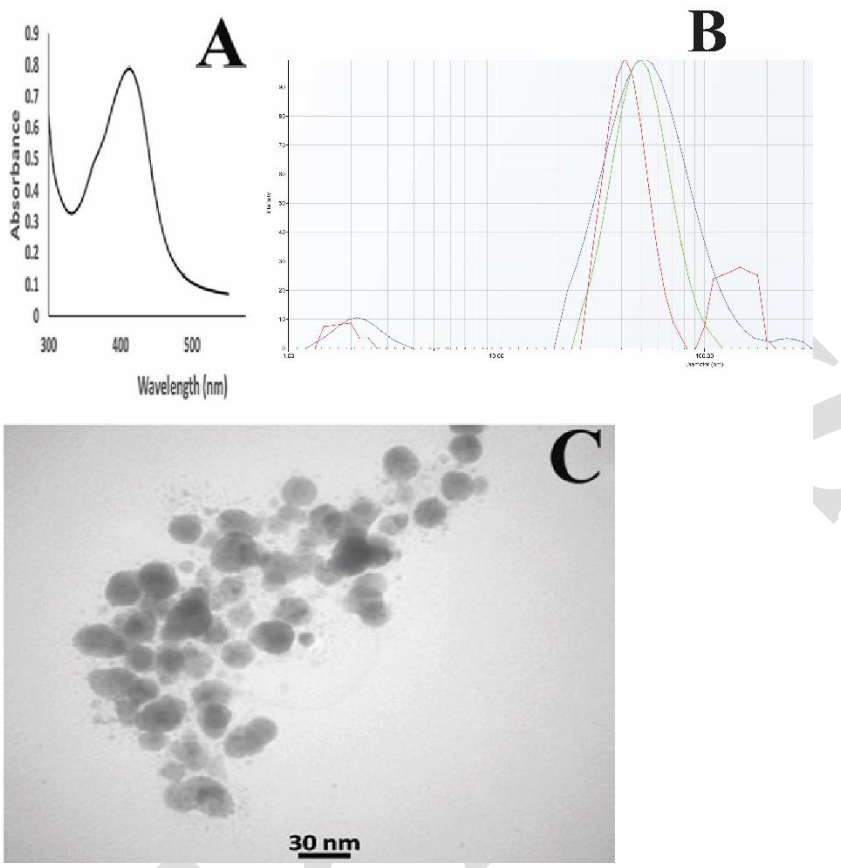

<Fig.1>

[DOI: 10.22068/ijmse.4109]

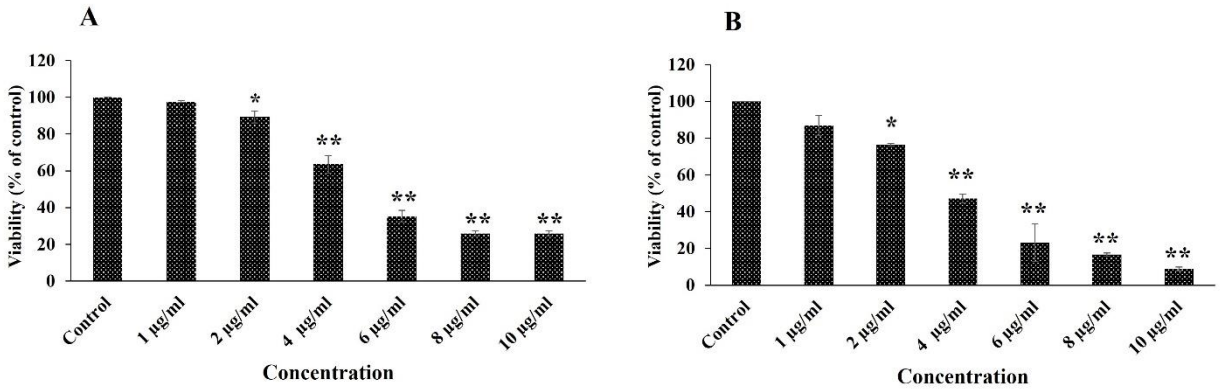

<Fig. 2>

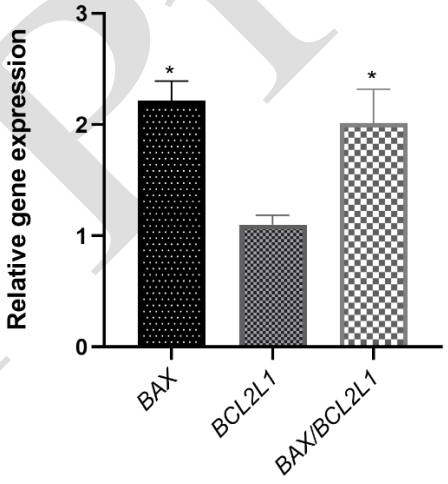

<Fig. 3>

[DOI: 10.22068/ijmse.4109]

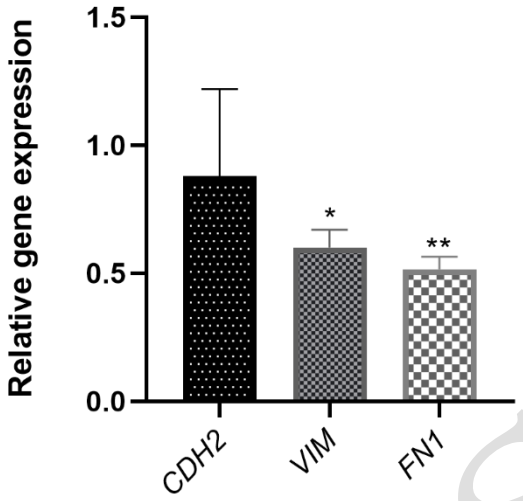

<Fig. 4>

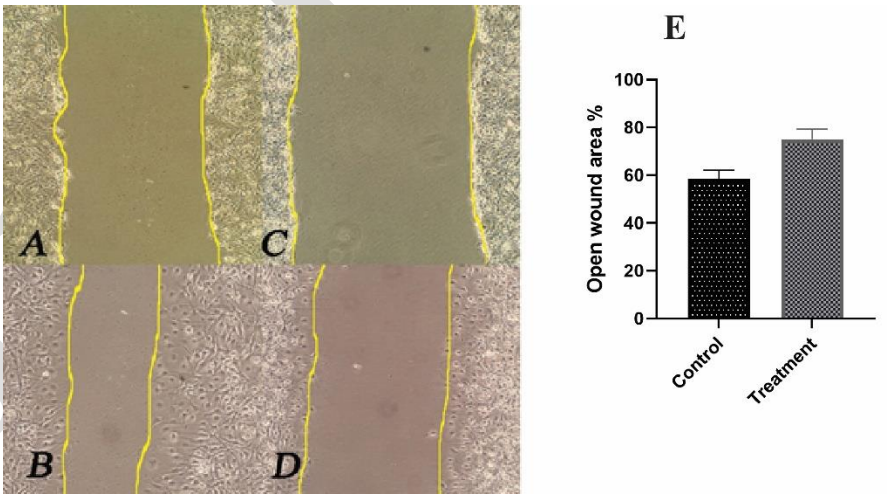

<Fig. 5>

[DOI: 10.22068/ijmse.4109]

[DOI: 10.22068/ijmse.4109]